Geochemistry Geophysics Geosystems G3
AN ELECTRONIC JOURNAL OF THE EARTH SCIENCES
Published by AGU and the Geochemical Society

Article
Volume 10, Number 11
21 November 2009
Q11013, doi:10.1029/2009GC002779
ISSN: 1525-2027

Preservation state of metastable magnesian calcite in periplatform sediments from the Caribbean Sea over the last million years

Sophie Sepulcre, Kazuyo Tachikawa, Laurence Vidal, Nicolas Thouveny, and Edouard Bard
CEREGE, UMR 6635, Aix-Marseille Université, Collège de France, CNRS, Europôle de l'Arbois, BP80, F-13545 Aix-en-Provence, France (sepulcre@cerege.fr)

[1] Carbonate-rich periplatform sediments represent an active carbon reservoir containing metastable aragonite and magnesian calcite (Mg-calcite, > 4 mol % $MgCO_3$). Since Mg-calcite is highly soluble, the preservation state of this mineral provides information on past carbonate systems at water depths shallower than the lysocline. The mineralogy and geochemistry of the carbonate-rich fine fraction (<63 μm) was determined for the last 940 ka in a sediment core collected from the Walton Basin (Northern Caribbean Sea, 846 m water depth). Mg/Ca ratios for Mg-calcite showed clear glacial-interglacial cycles with high values (12 mol % $MgCO_3$) during interglacials. Glacial Mg/Ca ratios were approximately 8 mol % $MgCO_3$ for the period from 940 ka to 400 ka, and approximately 10 mol % $MgCO_3$ for the last 400 ka. The Mg/Ca shift is concomitant with a preferential loss of Mg-calcite relative to aragonite. The preservation state of Mg-calcite revealed that the bottom water mass of the studied site was slightly more corrosive for the earlier period, possibly relating to a composition change in intermediate water and/or to the ventilation rate in the Atlantic Ocean.

Components: 8672 words, 7 figures.

Keywords: Mg-calcite preservation state; Mg/Ca in Mg-calcite; Caribbean Sea; mid-Pleistocene.

Index Terms: 0473 Biogeosciences: Paleoclimatology and paleoceanography (3344, 4900); 1065 Geochemistry: Major and trace element geochemistry.

Received 13 August 2009; **Revised** 21 September 2009; **Accepted** 28 September 2009; **Published** 21 November 2009.

Sepulcre, S., K. Tachikawa, L. Vidal, N. Thouveny, and E. Bard (2009), Preservation state of metastable magnesian calcite in periplatform sediments from the Caribbean Sea over the last million years, *Geochem. Geophys. Geosyst.*, *10*, Q11013, doi:10.1029/2009GC002779.

1. Introduction

[2] Calcium carbonates in marine sediments form a reactive carbon reservoir that plays an important role in the global carbon cycle [*Farrell and Prell*, 1989]. The accumulation of $CaCO_3$ in sediments is determined by a balance between biogenic $CaCO_3$ production in surface waters supersaturated with respect to carbonate minerals and dissolution in undersaturated waters at greater depths. The water depth at which the dissolution rate is equal to the rate of supply corresponds to the carbonate compensation depth (CCD). On the whole, $CaCO_3$ does not accumulate beneath the CCD, but $CaCO_3$ dissolution begins at a shallower water depth than the CCD. The critical level of carbonate undersaturation below which dissolution increases dramatically is called the lysocline, separating

sediments rich in $CaCO_3$ from sediments depleted in $CaCO_3$ [*Broecker and Clark*, 1999]. Since the $CaCO_3$ saturation state is mainly controlled by the carbonate ion concentration [CO_3^{2-}] in bottom water, the lysocline generally covaries with bottom water [CO_3^{2-}] [*Broecker and Takahashi*, 1978; *Broecker*, 2003]. Therefore, $CaCO_3$ dissolution is closely associated with the global mass balance of $CaCO_3$, ocean circulation, and the atmospheric CO_2 content, which are a part of global climate change [*Farrell and Prell*, 1989; *Broecker*, 2003]. For example, bulk $CaCO_3$ content in deep-sea sediments varies with glacial-interglacial cycles in global deepwater circulation [*Berger*, 1976; *Farrell and Prell*, 1989; *Bickert and Wefer*, 1996; *Archer and Martin*, 2001]. Several studies have revealed that the recent increase in atmospheric CO_2 has had a profound impact on the oceanic carbonate system at shallow water depths of 500 to 1000 m [*Sabine et al.*, 2004; *Feely et al.*, 2004; *Ridgwell and Hargreaves*, 2007; *Ridgwell et al.*, 2007].

[3] In contrast to deep-sea carbonate oozes that are essentially composed of calcite, carbonate-rich periplatform sediments contain metastable aragonite and magnesian calcite (Mg-calcite, > 4 mol % $MgCO_3$) [*Schlager and James*, 1978]. Since metastable minerals are more soluble than calcite [e.g., *Morse and Arvidson*, 2002] the preservation state of aragonite and Mg-calcite may yield supplementary information on the carbonate system at depths shallower than the lysocline [*Haddad and Droxler*, 1996]. *Droxler et al.* [1983] proposed using aragonite proportions as a means for reconstructing carbonate system evolution in thermocline and intermediate water depths in the Northern Bahamas during the late Pleistocene. However, the aragonite proportion of periplatform sediments is largely influenced by the neritic production rate, which is very sensitive to sea level changes. Therefore, it has been difficult to distinguish the dissolution effect from aragonite production variability at glacial-interglacial timescales [*Glaser and Droxler*, 1993; *Haddad and Droxler*, 1996].

[4] Mg-calcite in periplatform sediments is derived from the skeletons of organisms such as red algae, benthic foraminifera, and sea urchins, as well as the direct precipitation of marine cements [*Morse et al.*, 2006]. The solubility of Mg-calcite increases with Mg content, and biogenic Mg-calcite is more soluble than synthetic Mg-calcite [*Bischoff et al.*, 1983, 1987; *Paquette and Reeder*, 1990]. In modern marine environments, Mg-calcite with > 11 mol % $MgCO_3$ is more sensitive to dissolution than aragonite [*Morse et al.*, 2006]. Therefore, by combining the abundance and Mg content (Mg/Ca ratio) of Mg-calcite, we can gain some insight into subtle changes in the carbonate system at water depths shallower than the lysocline. However, few studies have applied this approach when reconstructing past carbonate systems [*Malone*, 2000; *Malone et al.*, 2001].

[5] Here, we focus on Mg-calcite in periplatform sediments collected from the Walton Basin, Northern Caribbean Sea, and attempt to use the combination of Mg/Ca and the abundance of Mg-calcite to study the evolution of a carbonate system at a water depth shallower than the lysocline (850 m) over the past 940 ka (covering the Mid-Pleistocene climate transition).

2. Sedimentary and Modern Hydrologic Settings

2.1. Origin of Sediments

[6] Core MD03–2628 was recovered in 2003 from the Walton Basin (17°21.26N, 77°42.45W, 846 m water depth, Figures 1a and 1b) during the IMAGES MD132 expedition. The Walton Basin, located in the northeastern part of the Nicaragua rise that separates the western and eastern parts of the Caribbean Sea, consists of a deep seaway between the Jamaican shelf and the Pedro Bank with water depths ranging between 200 and 2000 m (Figure 1b), and corresponds to a rather oligotrophic area with no active coastal upwelling [*Glaser and Droxler*, 1991; *Glaser*, 1992].

[7] Walton Basin sediments are typically periplatform oozes mainly composed of $CaCO_3$ phases [*Schlager and James*, 1978] with minor inputs (5–30%) of fine siliciclastics from Jamaica [*Glaser and Droxler*, 1991] (see also Figure S1[1]). The enclosed physiography of the basin favors the accumulation of fine fraction sediments (defined here as the fine-grained fraction < 63 μm), which contrasts with the southern and eastern Caribbean Sea where winnowing by Caribbean current prevents efficient accumulation of fine particles (Figure 1a). The fine carbonate fraction is composed of pelagic calcite, slope-derived biogenic aragonite and Mg-calcite, and possibly Mg-calcite formed by in situ cementation [*Moberly*, 1968;

[1]Auxiliary materials are available at ftp://ftp.agu.org/apend/gc/2009gc002779.

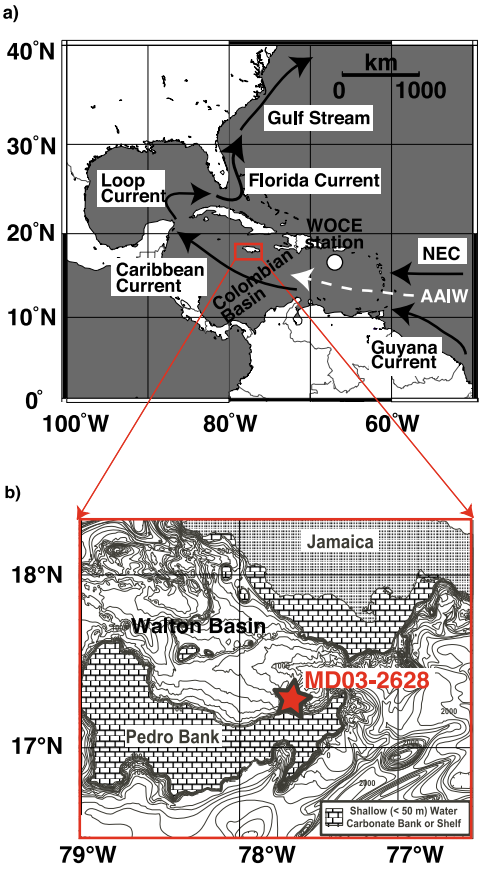

Figure 1. Location of the Walton Basin (red square) and of core MD03–2628 (17°21.26N, 77°42.45W, 846 m water depth) in the Caribbean Sea. (a) Surface currents (black arrows, North Equatorial Current (NEC)) and Antarctic Intermediate Water (AAIW) flow to the Caribbean Sea (white dotted arrow). The carbonate saturation state (Figure 3) was calculated using data from the WOCE station at 17°N and 66°W (white circle) (from http://www.aquarius.geomar.de). (b) A bathymetric map of the Walton Basin (reprinted from *Reijmer and Andresen* [2007], copyright 2007, with permission from Elsevier) showing the core (MD03–2628) location (red star).

Schlager and James, 1978; *Glaser and Droxler*, 1993]. Producers of the fine calcite are likely coccolithophorids (pelagic algae) and juvenile foraminifera with the neritic green algae *Halimeda* being the main source of fine aragonite [*Glaser and Droxler*, 1993; *Stanley and Hardie*, 1998]. The main source of biogenic Mg-calcite are coralline algae mixed with fragments of various organisms (e.g., benthic foraminifera, echinoderms) from neritic environments [*Moberly*, 1968; *Schlager and James*, 1978; *Glaser and Droxler*, 1993]. Modern surface sediment is composed of 70% aragonite, 15% Mg-calcite, and 15% calcite [*Glaser and Droxler*, 1991].

2.2. Caribbean Hydrography and Water Masses at the Core Site

[8] Caribbean surface water (0–50m) flows from the southeast toward the northwest together with the Caribbean current (Figure 1a) [*Wüst*, 1964; *Tomczak and Godfrey*, 2003]. The water mass is formed from the mixing of South Atlantic waters transported by the Guyana Current, and equatorial waters from the North Equatorial Current (Figure 1a) [*Schmitz and Richardson*, 1991]. The mean annual surface water temperature and salinity are 27.8°C and 35.8 p.s.u., respectively (Figure 2). Sub-Tropical Underwater underlies the surface water between 50 and 300 m. The water mass originates from the Sargasso Sea and is characterized by a salinity maximum of 36.7 p.s.u. (Figure 2) [*Morrison and Nowlin*, 1982]. Antarctic Intermediate Water (AAIW) is found at 300 to 1000 m, and can be identified by a salinity lower than 35.5 p.s.u.

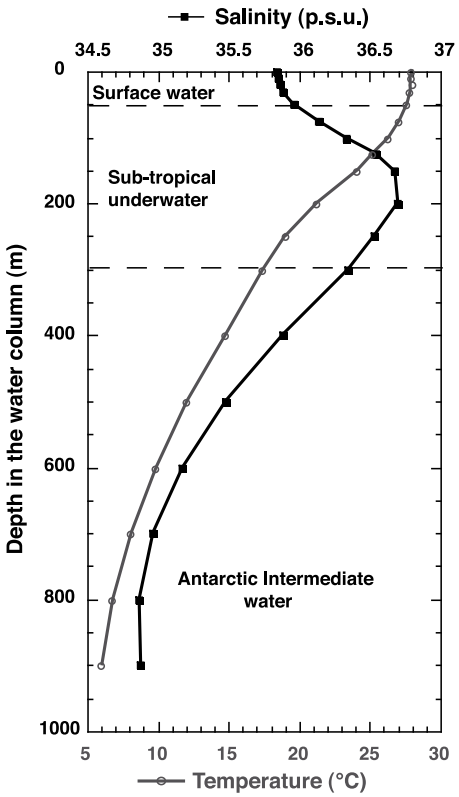

Figure 2. Depth profiles of present-day annual temperature (gray line and open symbols) and salinity (black line and squares) at 17.5°N 77.5°W [*Levitus and Boyer*, 1994]. Water masses flowing at the core site are also reported (see text for details).

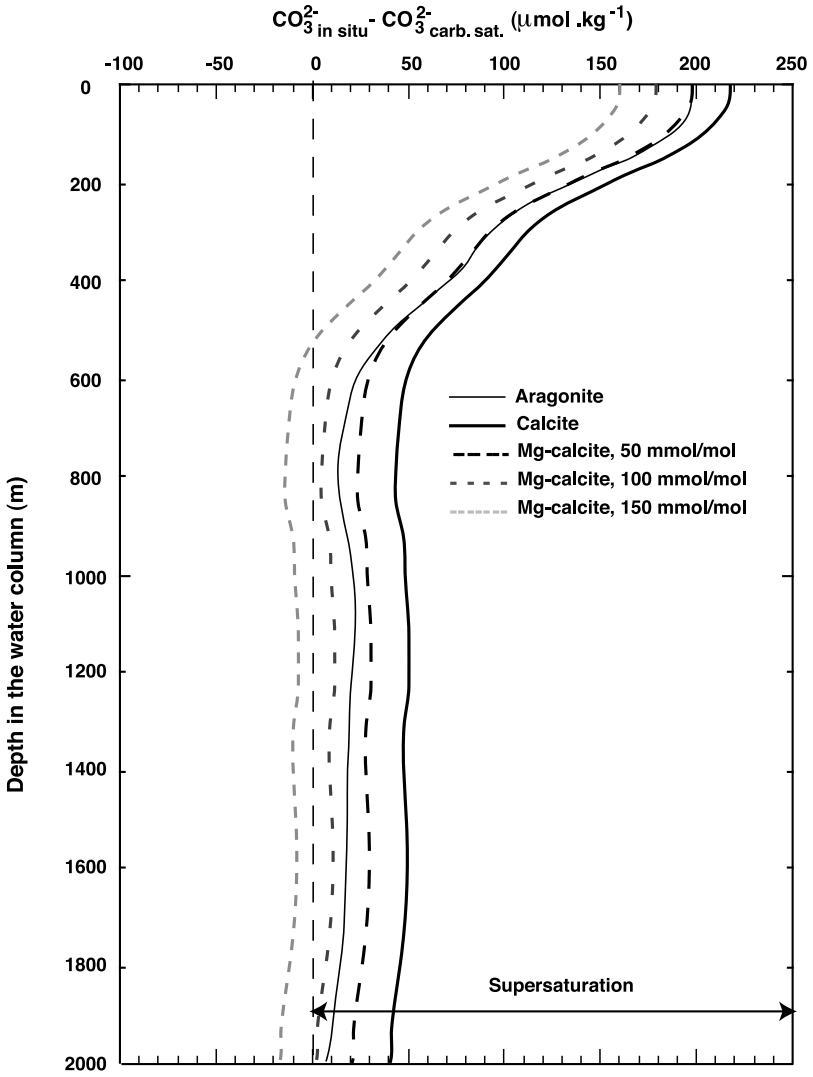

Figure 3. Depth profiles of the present-day carbonate saturation state ΔCO_3^{2-} (difference between $[CO_3^{2-}]_{in\ situ}$ and $[CO_3^{2-}]_{carbonate\ saturation}$) at WOCE station (17°N 66°W, Figure 1a) in the northern Caribbean Sea for calcite, aragonite, and Mg-calcite with various Mg/Ca values: Mg/Ca = 50 mmol/mol (4.8 mol % $MgCO_3$), 100 mmol/mol (9 mol % $MgCO_3$), and 150 mmol/mol (13 mol % $MgCO_3$) mmol/mol. ΔCO_3^{2-} values for calcite and aragonite were directly calculated using the CO2SYS software (E. Lewis and D. Wallace, CO2SYS.EXE, Program developed for CO2 system calculations, Brookhaven National Laboratory and Institut für Meereskunde, 2000, available at http://cdiac.esd.ornl.gov/oceans/co2rprt.html) and filed data from the WOCE station (salinity, temperature, pressure, silicate, and phosphate concentrations, as well as using total alkalinity and total inorganic CO_2). For Mg-calcite, ΔCO_3^{2-} was estimated using the equation proposed by *Brown and Elderfield* [1996], taking into account the Mg/Ca ratio: $\Delta CO_3^{2-} = \Delta(CO_3^{2-})_{Mg\ =\ 0} - 0.39*Mg/Ca$ (mmol/mol).

(Figure 2) [*Wüst*, 1964; *Fratantoni et al.*, 1997]. AAIW enters the Caribbean Sea almost exclusively through the eastern passage (Figure 1a) [*Tomczak and Godfrey*, 2003]. Along its path through the Caribbean Sea, AAIW is mixed with deep and CO_2-enriched waters from the Colombian Basin that upwells along the Nicaragua Rise [*Droxler et al.*, 1991]. Bottom seawater temperatures (around 900 m) close to the core site are roughly 6°C (Figure 2). Below 1000 m, the Caribbean Sea is occupied by Upper North Atlantic Deep Water (UNADW) with a salinity of approximately 35 p.s.u. (not shown in Figure 2) [*Wüst*, 1964; *Fratantoni et al.*, 1997].

[9] The saturation state of calcite, aragonite, and Mg-calcite is expressed by the parameter $\Delta[CO_3^{2-}]$ (the difference between $CO_{3\,in\ situ}^{2-}$ and $CO_{3\,saturation}^{2-}$) [*McCorkle et al.*, 1995] (Figure 3). $\Delta[CO_3^{2-}]$ values for calcite and aragonite were directly computed using CO2SYS software (E. Lewis and D. Wallace, CO2SYS.EXE, Program developed for CO_2 system calculations, Brookhaven National

Laboratory and Institut für Meereskunde, 2000, available at http://cdiac.esd.ornl.gov/oceans/co2rprt.html) for a World Ocean Circulation Experiment (WOCE, see http://woce.nodc.noaa.gov/wdiu/) station at 17°N and 66°W close to the core site (Figure 1a). The saturation state of Mg-calcite with various Mg/Ca ratios was tentatively estimated using the equation proposed by *Brown and Elderfield* [1996] (see Figure 3 caption for detail). Obtained saturation profiles indicated that the water was supersaturated with respect to calcite and aragonite down to 2000 m (Figure 3). The saturation state of Mg-calcite is highly sensitive to the Mg content. At water depths of approximately 1000 m, undersaturation is nearly reached for aragonite and Mg-calcite with high Mg contents (Mg/Ca more than 100 mmol/mol or more than 9 mol % $MgCO_3$, Figure 3). The corrosive intermediate water mass corresponds to AAIW from the South Atlantic that has mixed with CO_2-rich Colombian Basin water during its passage in the Caribbean Sea [*Droxler et al.*, 1991]. Mg-calcite with a high Mg content (Mg/Ca of 150 mmol/mol or 13 mol % $MgCO_3$) has been estimated to be undersaturated below 500 m (Figure 3), consistent with the observed dissolution of Mg-calcite at depths below 500 m in the Caribbean Sea [*Droxler et al.*, 1991].

3. Methods

[10] Core MD03−2628 was sampled every 20 cm and wet-sieved to separate the <63 μm, 63−150 μm, and >150 μm fractions. All of the fractions were dried in an oven at 50°C. The fine fraction was ground in a mortar for better homogeneity before analysis. The planktonic foraminifer *Globigerinoides ruber* (white) (250−350 μm) was hand picked from the >150 μm fraction. All sample preparations and instrumental measurements were carried out at CEREGE.

[11] $\delta^{18}O$ measurements were performed on 5 to 10 individuals of *G. ruber* as well as on the fine fraction using a Finnigan Delta Advantage mass spectrometer directly coupled to an automatic carbonate preparation device calibrated on the international scale (Vienna Pee Dee Belemnite VPDB). Analytical precision of the method was checked against the regular standard analysis of NBS19, and was better than 0.04‰ for $\delta^{18}O_{VPDB}$ (1σ; n = 169).

[12] In order to refine core chronostratigraphy, a paleomagnetic study was conducted on the core depth interval from 2651 to 1797 cm (940 to 630 ka). We focused on the lower parts of the core with the aim of identifying the Brunhes-Matuyama (B/M) polarity reversal (778 kyr) as a main chronological marker. Natural and anhysteretic remanent magnetizations were measured using a DC SQUID magnetometer (2G-760R) equipped with an alternating field (AF) demagnetizer and a direct field coil system located inside a magnetically shielded room. The instrument had a noise level of $\sim 10^{-9}$.Am^2 and a spatial resolution (length of window recording more than 50% of the centered moment) of ~4 cm on the x and y axes and 6 cm on the z axis. Magnetizations were measured at 2-cm intervals on U channels subsampled in archived sections of the core. Demagnetization steps applied at 10 mT AF allowed us to remove a weak spurious viscous overprint and to isolate a stable single component of magnetization from 20 mT up to 40 mT.

[13] Bulk sediment carbonate content was determined from the total and organic carbon content in bulk sediments with a FISONS NA 1500 elemental analyzer [see *Verardo et al.*, 1990]. After the analysis of total carbon, inorganic carbon was removed with HCl (0.01 M). The uncertainty of the carbonate content determined by this method was estimated at 3% (1σ) [*Pailler and Bard*, 2002].

[14] Carbonate mineralogy was determined by X-ray diffraction (XRD) using peak area ratios [*Sepulcre et al.*, 2009]. A calibration equation for the aragonite/calcite mixture was established using 19 standards (0.3 to 95% calcite) made from pure aragonite (modern coral) and pure calcite (natural mineral). A calibration for the Mg-calcite/calcite mixture was established using 10 standards (5 to 90% calcite) made from the same calcite and modern coralline Mg-calcite (red algae, 12.5 mol % $MgCO_3$). Measurements were taken on a Philips PW 3710 diffractometer with a cobalt Kα tube at 40 kV and 40 mA, using a 0.05° step and a counting time of 10 s per step. Areas for the maximum peaks of aragonite, calcite, and Mg-calcite were calculated using the PC-APD program. Uncertainties for aragonite/calcite and calcite/Mg-calcite determinations were estimated from the scatter of the calibration curves, and are less than 5%.

[15] The mol % $MgCO_3$ of Mg-calcite was determined using a radiocrystallographic approach with XRD using the calibration obtained by *Goldsmith and Graf* [1958].

$$\%MgCO_3 = 1010.2 - 333.1 * d_{(hkl)} \quad (1)$$

The mol % $MgCO_3$ of Mg-calcite was proportional to the shift in lattice spacing (d_{hkl}) between a pure

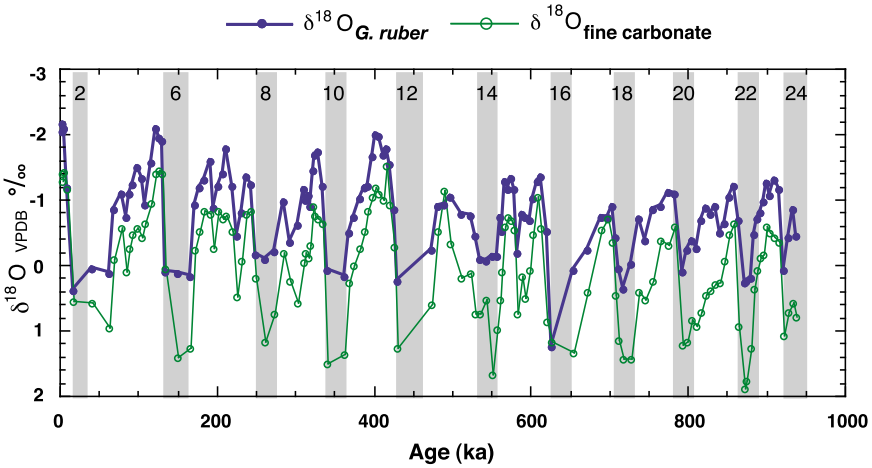

Figure 4. The $\delta^{18}O$ records of *Globigerinoides ruber* (bold blue line and solid circles) and the fine fraction (thin green curve and empty circles). Glacial marine isotopic stages determined by the foraminiferal $\delta^{18}O$ stratigraphy are shown with gray bars. The data are available as auxiliary material.

calcite and a Mg-calcite containing 0 to 50 mol % $MgCO_3$ (dolomite) [*Lumsden*, 1979]. The reproducibility of the method, estimated by replicate XRD analysis of a pure Mg-calcite standard, was better than 0.4 mol % $MgCO_3$.

4. Results

4.1. Core Chronological Framework

[16] The age model for core MD03–2628 was obtained by correlating the planktonic $\delta^{18}O$ record (Figure 4) with a reference record [*Lisiecki and Raymo*, 2005] using the Analyseries software [*Paillard et al.*, 1996] as well as the Brunhes-Matuyama reversal that was identified by paleomagnetic measurements (Figure S2). The record in core MD03–2628 extended down to Marine Isotope Stage (MIS) 24 that spans the last 940 ka. Sedimentation rates are highly variable from glacial to interglacial stages, with a constant trend of low to high values, respectively (Figure S2). On average, sedimentation rates for interglacial and glacial periods were determined as 4 and 2 cm/ka, respectively, with corresponding time resolutions of 5 ka and 10 ka, respectively (Figure S2).

[17] $\delta^{18}O$ values for *G. ruber* varied between −2.4 (interglacial) and 0.4‰ (glacial, except for MIS 16 at 1.2‰) for the last 600 ka (Figure 4). The results presented are in good agreement with previous planktonic $\delta^{18}O$ records from the Caribbean Sea [*Wolff et al.*, 1998; *Schmidt et al.*, 2004, 2006]. Amplitudes in glacial-interglacial $\delta^{18}O$ variations increased over the last 600 ka. Glacial and interglacial $\delta^{18}O$ values of the fine fraction were systematically higher than *G. ruber* values by approximately 0.8‰ and ranged from −1.5 to 1.9‰. Amplitudes of glacial-interglacial changes were approximately 2‰ and constant for the last 940 ka (Figure 4). $\delta^{18}O$ profiles for *G. ruber* and the fine fraction varied in phase at the temporal resolution studied here. The synchronicity was noteworthy since the chronostratigraphy was mainly established using the planktonic foraminiferal $\delta^{18}O$ record of the coarse fraction (>150 μm), while this study focused on the fine fraction (<63 μm). Indeed, we observed a slight phase lag in the $\delta^{18}O$ records between the two fractions during the last deglacial period at a finer-scale temporal resolution (0.3 ka and 3 ka during interglacial and glacial stages, respectively). The offset is partly explained by bioturbation [*Sepulcre et al.*, 2007].

[18] At the core MD03–2628 latitude (17°21.26N), variations in paleomagnetic vector inclinations due to a reversal in the normal transition of a purely dipolar field should be from −31.4° to +31.4°. Meanwhile, the NRM inclination recorded between 2700 and 1800 cm consisted of short wavelength oscillations of 20 to 40° in amplitude, superimposed on longer wavelength variations of 60 to 80° in amplitude (Figure 5b). Although the inclination was dominantly negative below 2200 cm and dominantly positive above 2000 cm, large amplitude oscillations, due to nondipole effects, precluded us from precisely defining the depth at which the polarity reversal was recorded. Therefore, we used relative paleointensity variations to identify the succession of dipole lows linked with the B/M transition and with excursions reported in the 900–600 kyr time interval. NRM intensity (Figure 5c) was normalized

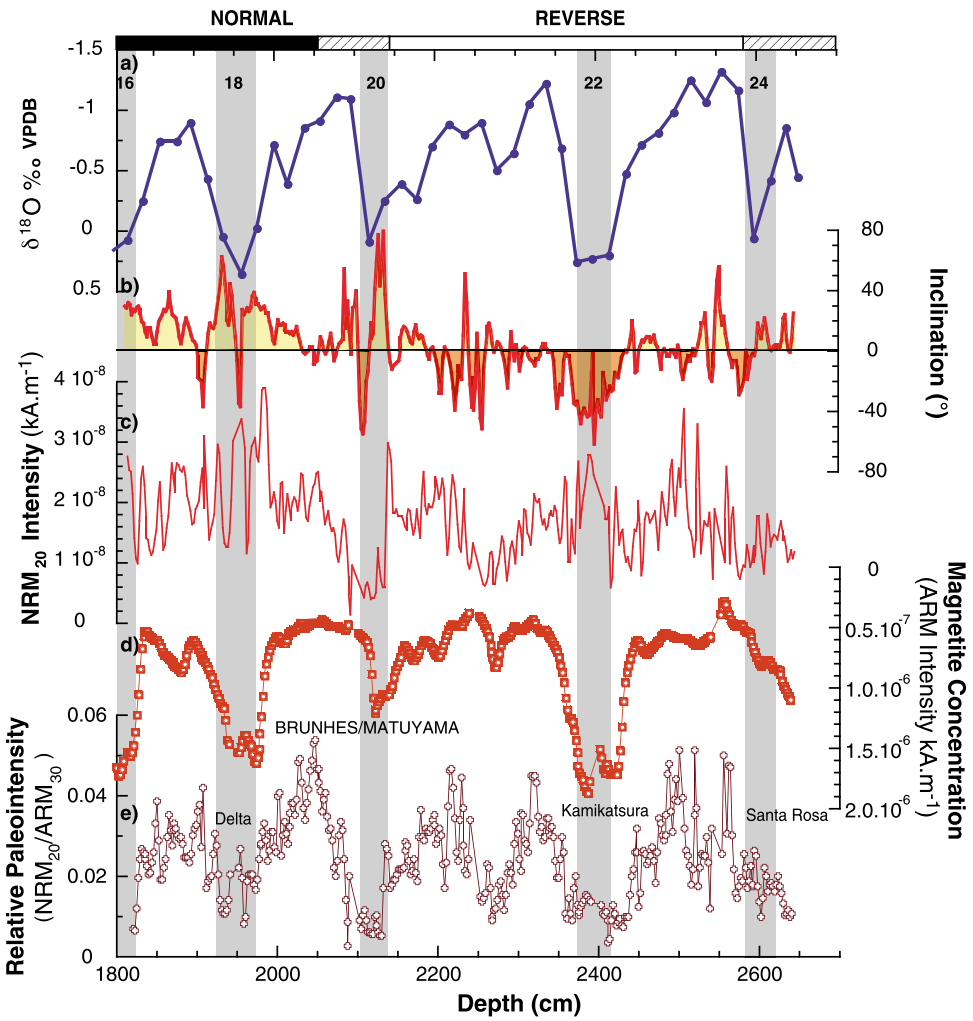

Figure 5. Paleomagnetic stratigraphy for the lower part of core MD03−2628. (a) Details of the $\delta^{18}O$ profile for *Globigerinoides ruber* (bold blue line and solid circles). (b) The inclination (thick red line) and (c) intensity (thin red line) of natural remanent magnetization (NRM). Variations of the NRM inclination between 2700 and 1800 cm consisted of shifts from a negative to a positive inclination as indicated by light orange and yellow areas, respectively, resulting either from magnetic reversals or from excursions or even from large amplitude secular variations. Therefore, declination shifts are more reliable and are made up of a progressive 180° declination change accompanied by a change in the sign of the inclination. However, these shifts are enhanced by large relative paleointensity (RPI) changes that accompany polarity transitions and excursions. (d) Anhysteretic remanent magnetization (ARM) as a proxy for magnetite concentration (white circles on red squares and thin red curve, *y* axis scale inverted in order to visually match $\delta^{18}O$ variations). In the Caribbean Sea, the detrital magnetic fraction appears to be essentially of volcanic origin and consists of titanomagnetite ($Fe_{3-x}Ti_xO_4$). The fact that fluctuations in anhysteretic remanent magnetization (ARM) mimic the $\delta^{18}O$ variations strongly suggests that the input of the magnetic fraction is controlled by erosion, river transport, and sea level variations (i.e., paleoclimatic changes). The magnetic fraction is more abundant during glacial episodes than during interglacial episodes, when it is diluted by the biogenic carbonate fraction. (e) The relative paleointensity given by the NRM intensity and normalized by the ARM intensity (brown thin line and crosses). The polarity transition recorded here, which can be attributed to the Brunhes-Matuyama (B/M) reversal, occurred at the same depth as the transition between marine isotope stages (MIS) 19 and 20 as defined by the $\delta^{18}O$ record. The B/M transition is known to have occurred during or at the end of the interglacial MIS 19 [*Bassinot et al.*, 1994; *Raisbeck et al.*, 2006]. However, in porous carbonate-rich sediments, the postdepositional remanent magnetization is often observed to be "locked in" at depths of 20 to 30 cm. The data are available as auxiliary material.

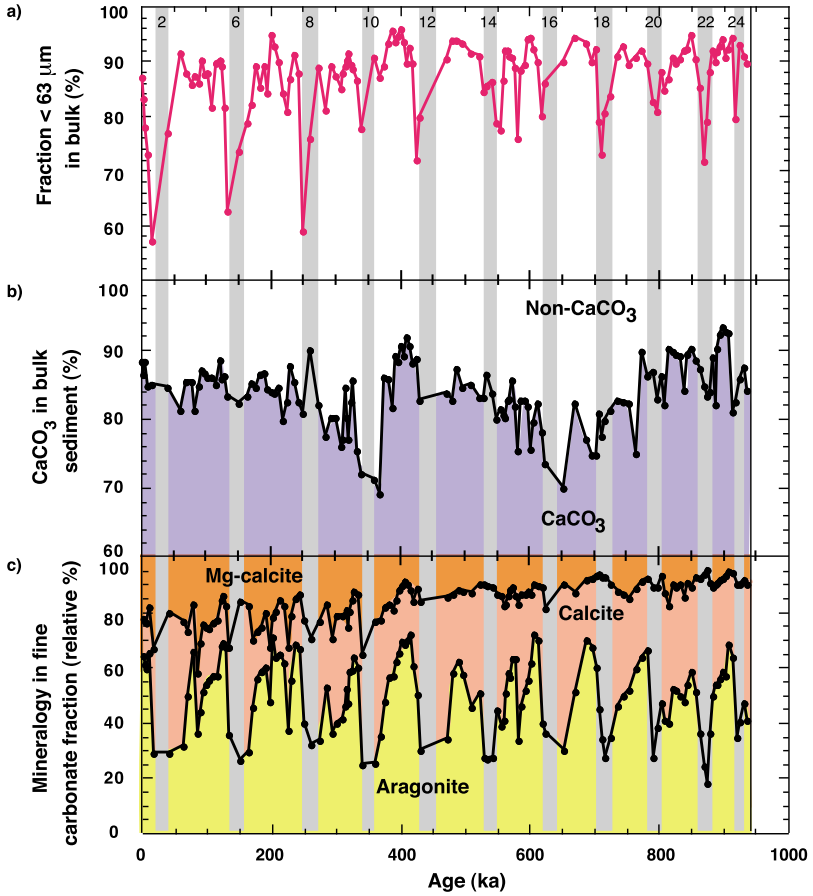

Figure 6. Variations in the chemical and mineralogical composition of sediments: (a) The abundance of the fine fraction in bulk sediment (pink bold line and solid circles). (b) The carbonate content in bulk sediment (light purple area and black line) calculated from the total carbon and the organic carbon content according to the relation given by *Verardo et al.* [1990]: % carbonates = 8.33*(Total Carbon − Organic Carbon). (c) The relative proportions of aragonite (yellow area), calcite (light orange area), and magnesian calcite (Mg-calcite, dark orange area) in the fine carbonate fraction. Marine Isotope Stages are the same as in Figure 4. The data are available as auxiliary material.

using the anhysteretic remanent magnetization (ARM) (Figure 5d) that was proportional to the concentration of pseudo single to small multidomain (0.1–10 μm) ferrimagnetic (Ti-magnetite) grains and that represents the most appropriate normalization parameter for reconstructing relative paleointensity (RPI) changes (Figure 5e). The deepest RPI low was recorded between 2140 and 2080 cm, and was framed by a progressive decrease from 2200 to 2140 cm, followed by a rapid increase from 2080 to 2040 cm (Figure 5e). Such an asymmetrical shape has often been reported in transitional dipole moment records [e.g., *Valet et al.*, 2005]. Therefore, the B/M polarity transition was exactly recorded between 2140 and 2080 cm (i.e., at the depth of the transition between MIS 20 and MIS 19) as defined by the δ^{18}O record (Figure 5a). A comparison of the MD03–2628 RPI curve (Figure 5e) with a reference record [*Carcaillet et al.*, 2003] allowed us to identify other RPI lows at approximately 2600, 2400, and 1950 cm, that were attributable to the Santa Rosa dipole low (910–920 ka BP), the Kamikatsura dipole low (880 ka BP), and the Delta dipole low (700 ka BP), respectively. Paleomagnetic results thus confirmed the δ^{18}O stratigraphy of core MD03–2628 over the time interval from 940 to 630 ka.

4.2. Mineralogy and Geochemistry of the Fine Carbonate Fraction

[19] The proportion of the fine fraction in bulk sediment exhibits remarkable glacial-interglacial cycles (Figure 6a). Over the entire record, interglacial values are higher than glacial values, with an average of approximately 90% from MIS 24 to MIS 11, and approximately 85% from MIS 9 to the

core top. The glacial fine fraction proportion shows a shift at approximately 400 ka from an average value of 75% between MIS 24 and MIS 10 to approximately 60% between MIS 8 and MIS 2 (Figure 6a). A similar trend is observed for the interglacial stages, with average values higher than 90% from MIS 23 to MIS 11 and lower than 90% from MIS 9 to the core top (Figure 6a).

[20] The carbonate content in the bulk sediment varied between 70 and 93% without any clear glacial-interglacial variability (Figure 6b). The record displayed a low-frequency cycle with maximum carbonate values centered at 940 ka and nearly 400 ka. The noncarbonate fraction is a minor component corresponding to siliciclastic material, consistent with the results of a previous study [*Glaser and Droxler*, 1993].

[21] The fine carbonate fraction is the major constituent of bulk sediment. Its core top composition is 65% aragonite, 15% calcite, and 20% Mg-calcite (Figure 6c) in good agreement with the mineralogical composition of modern carbonates in the Walton Basin [*Glaser and Droxler*, 1991]. The aragonite content in the core varied between 72 and 18%, exhibiting a well-developed cyclicity with an abrupt increase at glacial-interglacial transitions followed by a gradual decrease to lower glacial values (Figure 6c). The glacial-interglacial amplitude of the aragonite content remained almost constant throughout the record. The calcite content mirrored the aragonite variations, ranging from 7% (interglacials) to 77% (glacials) (Figure 6c). Superimposed on the glacial-interglacial cyclicity, we observed a long-term gradually decreasing trend between 40% at 940 ka and 27% at 400 ka. The Mg-calcite content ranged from 4 to 42% over the entire record, with a higher average value of 22% for the last 400 ka than for the older part of the profile (11%) (Figure 6c).

[22] The mol % $MgCO_3$ in Mg-calcite determined by XRD ranged from 7.5 to 12.5% over the entire core (corresponding to Mg/Ca values of 80 to 145 mmol/mol), indicating a very clear glacial-interglacial variability (Figure 7a). The Mg/Ca values were systematically higher during interglacial periods with an average value of approximately 12 mol % $MgCO_3$ over the entire record except for MIS 11 where a sharp decrease of Mg/Ca to 10 mol % $MgCO_3$ was observed at roughly 400 ka. Glacial values ranges from 7 to 9 mol % $MgCO_3$ from MIS 24 to MIS 14, and were slightly higher around 10 mol % $MgCO_3$ between MIS 12 and MIS 2, apart from a low value of 8 mol % $MgCO_3$ at MIS 10.

5. Discussion

[23] Except for the proportion of fine aragonite, which followed a similar trend to glacial-interglacial $\delta^{18}O$ variations over the entire core, the fine fraction generally indicated a change in the sedimentary regime at approximately 400 ka (Figures 6a, 6c, and 7a). In the following paragraphs, we discuss some potential factors influencing Mg-calcite abundance. Then, we propose a possible link between the preservation state of metastable carbonates and a change in the nature and/or the ventilation rate of bottom water at the studied site in relation to intermediate water in the Atlantic Ocean.

[24] Our interpretation was based on the relative abundances presented above (Figure 6c) since absolute mass accumulation rates (MAR) did not provide supplementary information, as the results followed the changes observed in relative abundances. Additionally, MAR are difficult to assess precisely for the core MD03–2628 case. In order to calculate MAR one needs sedimentation rates as well as the bulk sediment density, and the later was not available for core MD03–2628. We attempted to calculate MAR by estimating bulk sediment density using the proportion and the bulk density of fine calcite, fine aragonite, fine Mg-calcite, the noncarbonate fraction, and the coarse fraction. However, the calculation did not constitute an absolute quantification of MAR and was strongly influenced by chosen values of densities, in particular for Mg-calcite, where the density depends on the Mg amount, and the noncarbonate and the coarse fractions, which are mixtures of various components. Therefore, below we discuss the relative abundances rather than MAR, for which values may be biased by the estimation of density values.

5.1. Influence of Cementation and Diagenesis on Mg-Calcite Abundance

[25] Biogenic Mg-calcite in periplatform sediments is mainly produced in neritic environments [*Moberly*, 1968; *Schlager and James*, 1978; *Glaser and Droxler*, 1993]. Higher productivity is expected during interglacial periods because the slope and shelf are submerged within the photic zone, thus enlarging the surface area available for neritic productivity [*Glaser and Droxler*, 1993]. In

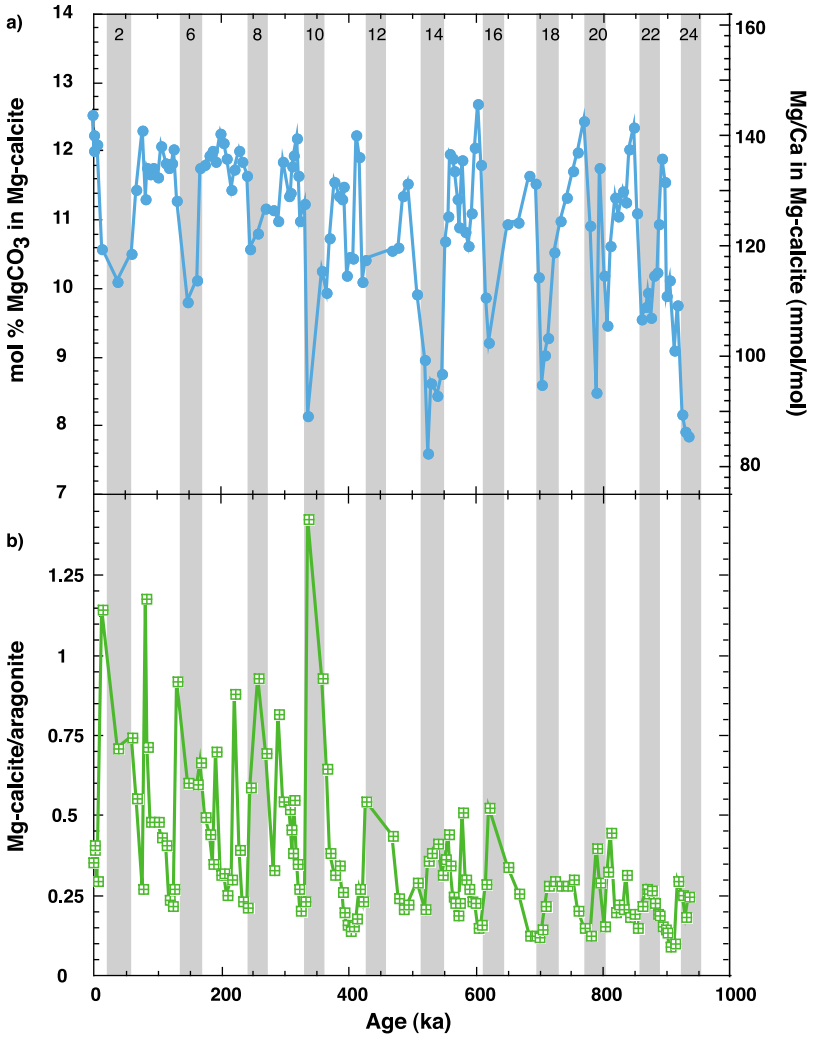

Figure 7. Records of metastable carbonate: (a) Mg content in Mg-calcite with mol % $MgCO_3$ and Mg/Ca (mmol/mol) as determined by X-ray diffraction (light blue line and solid circles). (b) Ratio of Mg-calcite to aragonite in the fine fraction (light green line and squares). Marine Isotope Stages are the same as in Figure 4. The data are available as auxiliary material.

fact, the proportion of aragonite and the bulk sedimentation rate are higher during interglacial periods, and this trend was maintained for the entire record (Figures 6c and S2), suggesting that neritic productivity was mainly controlled by sea level over the last 940 ka without any significant shift at approximately 400 ka. Mg-calcite abundance did not show clear glacial-interglacial cycles, possibly due to the dominant effect of dilution by aragonite. Besides productivity, cement formation and diagenetic processes (loss of Mg-calcite by dissolution in bottom waters) could have modified the abundance of Mg-calcite. Marine cement is produced at the sediment-water interface at water depths shallower than 1200 m close to carbonate platforms [*Schlager and James*, 1978]. The existence of cements can be detected by Mg/Ca ratios in Mg-calcite [*Moberly*, 1968; *Schlager and James*, 1978] since Mg incorporation into abiotic Mg-calcites is predominantly controlled by water temperature [*Burton and Walter*, 1987; *Mucci*, 1987; *Hartley and Mucci*, 1996]. Applying the relationship between water temperature and the Mg/Ca ratio of inorganic precipitates [*Oomori et al.*, 1987] to the observed Mg/Ca values of Mg-calcite (Figure 7a), the water temperature was estimated at 20 to 35°C. This temperature range is closer to present-day surface water temperatures (27.8°C) than to bottom water temperatures (6°C, Figure 2) indicating that Mg-calcite was principally formed in surface waters. If we apply the calibration between water temperature and the Mg/Ca ratio

of biogenic carbonates such as high-Mg, shallow water benthic foraminifera [*Toyofuku et al.*, 2000], or high Mg-calcite gorgonian [*Bond et al.*, 2005], the estimated temperatures vary between 10 and 25°C for glacial and interglacial stages, respectively (except for a few glacial stages where temperatures are lower than 10°C). The interglacial values are in good agreement with the modern temperature of 27.8°C, and the values calculated for glacial stages are again higher than bottom water temperature. Moreover, as part of the Mg-calcite produced during glacial periods may be of abiotic origin, due to higher hydrodynamical conditions that favors cement precipitation [*Glaser and Droxler*, 1993], the most appropriate calibration remains the relationship based on inorganic precipitates [*Oomori et al.*, 1987]. Therefore, variations in the Mg/Ca ratio of Mg-calcite are likely related to the biological influence on Mg incorporation rather than to real climate variability.

[26] Burial diagenesis could decrease Mg-calcite abundance in sediments by transforming Mg-calcite into more stable calcite during sediment compaction. We estimate that the influence of this process only has a minor influence in core MD03–2628 for the following reasons. First, burial diagenesis has a significant impact on extremely long cores (typically more than 30 m) [*Haddad and Droxler*, 1996; *Lyons et al.*, 2000; *Fantle and DePaolo*, 2006, 2007] whereas the entire length of core MD03–2628 was approximately 27 m and the core depth corresponding to 400 ka was only 12 m (Figure S2). Second, compaction should occur continuously with increasing core depth unless drastic changes in the nature of the sediments had occurred. While core MD03–2628 exhibited a relatively stable sedimentary composition (Figure 6b), we observed a sudden drop in Mg-calcite abundance at approximately 400 ka (Figure 6c). Finally, continuous burial diagenesis is incompatible with a sharp decrease for Mg/Ca ratios in Mg-calcite during glacial periods from 940 ka to 400 ka (Figure 7a). We consider that the influence of early diagenesis is negligible due to very low organic carbon concentrations in this core (0.08–0.5%) [*Sepulcre*, 2008].

[27] Therefore, the principal source of Mg-calcite is biogenic, whereas in situ cementation and diagenetic processes only have a limited influence. Hence, variability in Mg-calcite abundance could be explained by the preferential dissolution of this mineral in contact with bottom water at the core site, which corresponds to the intermediate water mass in the Caribbean Sea. This hypothesis is consistent with our overall data set. Mg-calcite may have been partly transformed into calcite (Figure 3). The transformation did not modify the total $CaCO_3$ content, consistent with the observed stable carbonate concentration in bulk sediment (Figure 6b). The proportion of the fine fraction in bulk sediment increased during glacial periods older than 400 ka (Figure 6a). Such an observation does not conflict with our hypothesis, if we take into account the progressive break up of coarse foraminiferal tests (>150 μm) [*Broecker and Clark*, 1999]. Even though foraminiferal tests are calcite, their porous structure makes them more soluble than pure calcite [*Dittert and Henrich*, 2000; *Loubere and Chellappa*, 2008; *Tachikawa et al.*, 2008].

5.2. Preservation State of Metastable Carbonate Minerals and the Change in Carbonate Ion Concentrations at Intermediate Water Depths in the Caribbean Sea

[28] We examined the extent of the change in carbonate ion concentrations in bottom water at the studied site by comparing Mg-calcite and aragonite abundances, and by taking into account the distinct sensitivity of these metastable minerals to carbonate ion concentrations (Figure 3). The abundance ratio of Mg-calcite to aragonite in the fine fraction seemed to shift at approximately 400 ka, which suggests a preferential loss of Mg-calcite during glacial periods between 940 and 400 ka (Figure 7b). The inferred change in the carbonate ion concentration at intermediate water depths in the Caribbean Sea is subtle since aragonite did not show any clear evidence for dissolution over the entire record (Figure 6c). We tentatively estimated the order of magnitude for this change by assuming that the mean glacial Mg/Ca values in Mg-calcite were 90 mmol/mol and 110 mmol/mol for 940–400 ka and the last 400 ka, respectively (Figure 7a). We also hypothesize that the change in the calcite saturation state was negligible at the studied site over the past 940 ka, and that the Mg-calcite saturation state is expressed with the following equation for the studied period: $\Delta CO_3^{2-} = \Delta(CO_3^{2-})_{Mg=0} - 0.39*Mg/Ca$ (mmol/mol) [*Brown and Elderfield*, 1996] (Figure 3). The estimated change in the carbonate ion concentration is effectively small, on the order of 8 μmol/kg, in good agreement with our observations. Worth emphasizing is that this change occurred under the condition of calcite supersaturation, and can be evaluated uniquely using metastable Mg-calcite.

[29] Several mechanisms may explain the subtle changes in the carbonate ion concentration in the bottom water at the studied site. At present, the bottom water at the core site corresponds to AAIW, more corrosive (lower $[CO_3^{2-}]$) than the water masses of northern origin such as UNADW (Figures 2 and 3). Hence, increased dissolution during glacial periods between 940 and 400 ka observed in core MD03–2628 results cannot be explained by the predominant contribution of northern origin water masses. Therefore, changes occurred inside the AAIW water mass. Potential candidates for explaining the slightly more corrosive AAIW are multiple, including: 1) modifications in nature, 2) productivity changes in the pathway of this intermediate water from formation areas to the Walton Basin, and 3) changes in the ventilation rate of the water mass entering the Caribbean Sea. A modification in the nature of the AAIW (hypothesis 1) seems improbable since the contribution of nutrient-rich North Indian water to AAIW production is reduced during glacial periods [*Lynch-Stieglitz and Fairbanks*, 1994; *Peeters et al.*, 2004], opposite of the observed trend. Another hypothesis, based on variations in alkalinity and air-sea partitioning of CO_2 in intermediate water formation zones that may have an impact on the carbonate system of the source water, is possible. Hence, changes in the planktonic community (diatom versus coccolith) [e.g., *Dugdale et al.*, 2004], wind regime [e.g., *Toggweiler and Samuels*, 1998], and temperature in the AAIW formation zones can contribute to the observed modification although we have no clear evidence for the variations of these factors over the studied timescale. Under modern conditions, the carbonate ion concentration of AAIW does not really evolve from the source area to the Caribbean Sea [*Chung et al.*, 2003]. If this analogy to the modern condition was maintained for the studied period, the mechanism proposed as hypothesis 2 only has minor importance. Therefore, we propose that the reduced ventilation rate of intermediate water entering the Caribbean Sea and a consequent increase in the contribution of CO_2-rich Colombian Basin water to AAIW inside of the Caribbean Sea (hypothesis 3) is the probable reason.

[30] During glacial periods, the extension of sea ice around Antarctica and its northward transport modifies the freshwater budget at southern high latitudes, leading to saltier and denser AAIW and Antarctic Bottom Water (AABW) than the NADW [*Keeling and Stephens*, 2001]. The density contrast greatly influences global ocean circulation with reduced intermediate and deep ventilation [*Keeling and Stephens*, 2001]. In the Caribbean Sea, reduced AAIW circulation during glacial periods has already been observed [*Oppo and Fairbanks*, 1990], consistent with our hypothesis. At longer timescales, even though the deep and intermediate ocean circulation pattern between 940 ka and 400 ka is poorly known, the weaker production of AABW between 860 ka and 450 ka has been suggested from a marine core in the Southwestern Pacific [*Hall et al.*, 2001]. The decrease in AABW formation observed in the Pacific may be linked to a reduced AAIW ventilation as observed in core MD03–2628 results for the 940–400 ka time period.

[31] For the modern ocean, AAIW is considered as a critical carrier of salt and heat to the Arctic at intermediate depths, which in turn influences the formation of NADW [*Gordon et al.*, 1992]. Evidence for the crucial role of AAIW in past changes in oceanic circulation have been pointed out from modeling studies [*Keeling and Stephens*, 2001] and paleoceanographic records [*Peeters et al.*, 2004; *Pahnke and Zahn*, 2005]. The proposed change for AAIW ventilation rate in the Caribbean Sea may have a global impact, although our data set did not allow a precise evaluation for the change in the ventilation rate. Our study clearly indicates the potential usefulness of combining carbonate mineralogical composition with Mg/Ca in Mg-calcite for investigating subtle changes in the past carbonate system.

6. Conclusions

[32] We applied a combination of mineralogical and geochemical approaches in order to study periplatform sediments in core MD03–2628 from the Walton Basin of the Caribbean Sea over the last 940 ka. The abundance of fine (<63 μm) magnesian calcite (Mg-calcite) and the Mg/Ca ratio in Mg-calcite were coupled to gather more insight regarding subtle changes in the carbonate system at an intermediate water depth (850 m). At glacial-interglacial timescales, Mg/Ca ratios in Mg-calcite (>4 mol % $MgCO_3$) were higher (12 mol % $MgCO_3$) during interglacials than during glacials (8 to 10 mol % $MgCO_3$). At longer timescales, Mg/Ca ratios, the Mg-calcite to aragonite ratio in the fine fraction, as well as the abundance of the fine fraction in bulk sediment, suggest slightly corrosive intermediate water during glacial periods between 940 ka and 400 ka. A possible explanation for this change is a subtle reduction in the venti-

lation rate of AAIW in relation to global reorganization of oceanic circulation and a consequent increase in contributions of CO_2-rich water inside the Caribbean Sea. The change in carbonate ion concentrations is tentatively estimated at 8 μmol/kg and this change occurred under a calcite saturation condition. Therefore, our study emphasizes the potential usefulness of combining carbonate mineralogical composition with the chemical composition of metastable carbonates in order to investigate subtle changes in past carbonate systems at intermediate depths.

Acknowledgments

[33] Paleoclimate work at CEREGE is supported by the French MESR and the Collège de France, grants from the CNRS, the ANR-05-BLANC-0312-01, the Gary Comer Science and Education Foundation, the IMAGES program, and the European Community (Project Past4Future). We acknowledge André Droxler, Claude Hillaire-Marcel and Rosalind Rickaby for fruitful discussion. We are grateful to Corinne Sonzogni and Daniel Borschneck for technical help.

References

Archer, D., and P. Martin (2001), Ocean circulation—Thin walls tell the tale, *Science*, *294*, 2108–2109, doi:10.1126/science.1067168.

Bassinot, F., L. D. Labeyrie, E. Vincent, X. Quidelleur, N. J. Shackleton, and Y. Lancelot (1994), Astronomical theory of climate and the age of the Brunhes-Matuyama reversal, *Earth Planet. Sci. Lett.*, *126*, 91–108, doi:10.1016/0012-821X(94)90244-5.

Berger, W. H. (1976), Biogenous deep-sea sediments: Production, preservation and interpretation, in *Treatise on Chemical Oceanography*, vol. 5, edited by J. P. Riley and R. Chester, pp. 265–388, Academic, London.

Bickert, T., and G. Wefer (1996), Late Quaternary deep water circulation in the South Atlantic: Reconstruction from carbonate dissolution and benthic stable isotopes, in *The South Atlantic: Present and Past Circulation*, edited by G. Wefer et al., pp. 599–620, Springer, Berlin.

Bischoff, W. D., F. C. Bishop, and F. T. Mackenzie (1983), Biogenically produced magnesian calcite inhomogeneities in chemical and physical-properties comparison with synthetic phases, *Am. Mineral.*, *68*, 1183–1188.

Bischoff, W. D., F. T. Mackenzie, and F. C. Bishop (1987), Stabilities of synthetic magnesian calcites in aqueous-solution: Comparison with biogenic materials, *Geochim. Cosmochim. Acta*, *51*, 1413–1423, doi:10.1016/0016-7037(87)90325-5.

Bond, Z. A., A. L. Cohen, S. R. Smith, and W. J. Jenkins (2005), Growth and composition of high-Mg calcite in the skeleton of a Bermudian gorgonian (*Plexaurella dichotoma*): Potential for paleothermometry, *Geochem. Geophys. Geosyst.*, *6*, Q08010, doi:10.1029/2005GC000911.

Broecker, W. S. (2003), The oceanic $CaCO_3$ cycle, in *Treatise on Geochemistry*, vol. 6, edited by H. D. Holland and K. K. Turekian, pp. 529–549, Elsevier, London.

Broecker, W. S., and E. Clark (1999), $CaCO_3$ size distribution: A paleocarbonate ion proxy?, *Paleoceanography*, *14*, 596–604, doi:10.1029/1999PA900016.

Broecker, W. S., and T. Takahashi (1978), The relationship between lysocline depth and in situ carbonate ion concentration, *Deep Sea Res.*, *25*, 65–95.

Brown, S. J., and H. Elderfield (1996), Variations in Mg/Ca and Sr/Ca ratios of planktonic foraminifera caused by post-depositional dissolution: Evidence of shallow Mg-dependent dissolution, *Paleoceanography*, *11*, 543–551, doi:10.1029/96PA01491.

Burton, E. A., and L. M. Walter (1987), Relative precipitation rates of aragonite and Mg calcite from seawater—Temperature or carbonate ion control, *Geology*, *15*, 111–114, doi:10.1130/0091-7613(1987)15<111:RPROAA>2.0.CO;2.

Carcaillet, J. T., N. Thouveny, and D. L. Bourlès (2003), Geomagnetic moment instability between 0.6 and 1.3 Ma from cosmonuclide evidence, *Geophys. Res. Lett.*, *30*(15), 1792, doi:10.1029/2003GL017550.

Chung, S.-N., K. Lee, R. A. Feely, C. L. Sabine, F. J. Millero, R. Wanninkhof, J. L. Bullister, R. M. Key, and T.-H. Peng (2003), Calcium carbonate budget in the Atlantic Ocean based on water column inorganic carbon chemistry, *Global Biogeochem. Cycles*, *17*(4), 1093, doi:10.1029/2002GB002001.

Dittert, N., and R. Henrich (2000), Carbonate dissolution in the South Atlantic Ocean: Evidence from ultrastructure breakdown in *Globigerina bulloides*, *Deep Sea Res., Part I*, *47*, 603–620, doi:10.1016/S0967-0637(99)00069-2.

Droxler, A. W., W. Schlager, and C. C. Whallon (1983), Quaternary aragonite cycles and Oxygen-isotope record in Bahamian carbonate ooze, *Geology*, *11*, 235–239, doi:10.1130/0091-7613(1983)11<235:QACAOR>2.0.CO;2.

Droxler, A. W., J. W. Morse, K. S. Glaser, G. A. Haddad, and P. A. Baker (1991), Surface sediment carbonate mineralogy and water column chemistry: Nicaragua Rise versus the Bahamas, *Mar. Geol.*, *100*, 277–289, doi:10.1016/0025-3227(91)90236-W.

Dugdale, R. C., M. Lyle, F. P. Wilkerson, F. Chai, R. T. Barber, and T.-H. Peng (2004), Influence of equatorial diatom processes on Si deposition and atmospheric CO_2 cycles at glacial/interglacial timescales, *Paleoceanography*, *19*, PA3011, doi:10.1029/2003PA000929.

Fantle, M. S., and D. J. DePaolo (2006), Sr isotopes and pore fluid chemistry in carbonate sediment of the Ontong Java Plateau: Calcite recrystallization rates and evidence for a rapid rise in seawater Mg over the last 10 million years, *Geochim. Cosmochim. Acta*, *70*, 3883–3904, doi:10.1016/j.gca.2006.06.009.

Fantle, M. S., and D. J. DePaolo (2007), Ca isotopes in carbonate sediment and pore fluid from ODP Site 807A: The Ca^{2+}(aq)-calcite equilibrium fractionation factor and calcite recrystallization rates in Pleistocene sediments, *Geochim. Cosmochim. Acta*, *71*, 2524–2546, doi:10.1016/j.gca.2007.03.006.

Farrell, J. W., and W. L. Prell (1989), Climatic change and $CaCO_3$ preservation: An 800 000 years bathymetric reconstruction from the Equatorial Pacific ocean, *Paleoceanography*, *4*, 447–466, doi:10.1029/PA004i004p00447.

Feely, R. A., C. L. Sabine, K. Lee, W. Berelson, J. Kleypas, V. J. Fabry, and F. J. Millero (2004), Impact of anthropogenic CO_2 on the $CaCO_3$ system in the oceans, *Science*, *305*, 362–366, doi:10.1126/science.1097329.

Fratantoni, D. M., R. J. Zantopp, W. E. Johns, and J. L. Miller (1997), Updated bathymetry of the Anegada-Jungfern Passage complex and implications for Atlantic inflow to the Abyssal Caribbean Sea, *J. Mar. Res.*, *55*, 847–860, doi:10.1357/0022240973224148.

Glaser, K. S. (1992), Late Quaternary periplatform sediments and environments on the Northeastern Nicaragua Rise, Caribbean Sea, Ph.D. Thesis, 244 pp., Rice Univ., Houston, Tex.

Glaser, K. S., and A. W. Droxler (1991), High production and highstand shedding from deeply submerged carbonate banks, Northern Nicaragua Rise, *J. Sediment. Petrol.*, *61*, 128–142.

Glaser, K. S., and A. W. Droxler (1993), Controls and development of Late Quaternary periplatform carbonate stratigraphy in Walton Basin (Northeastern Nicaragua Rise, Caribbean Sea), *Paleoceanography*, *8*, 243–274, doi:10.1029/92PA02876.

Goldsmith, J. R., and D. L. Graf (1958), Relation between lattice constants and composition of the Ca Mg carbonates, *Am. Mineral.*, *43*, 82–101.

Gordon, A. L., R. F. Weiss, W. M. Smethie, and M. J. Warner (1992), Thermocline and intermediate water communication between the South Atlantic and Indian oceans, *J. Geophys. Res.*, *97*(C5), 7223–7240, doi:10.1029/92JC00485.

Haddad, G. A., and A. W. Droxler (1996), Metastable $CaCO_3$ dissolution at intermediate water depths of the Caribbean and western North Atlantic: Implications for intermediate water circulation during the past 200,000 years, *Paleoceanography*, *11*, 701–716, doi:10.1029/96PA02406.

Hall, I. R., I. N. McCave, N. J. Shackleton, G. P. Weedon, and S. E. Harris (2001), Intensified deep Pacific inflow and ventilation in Pleistocene glacial times, *Nature*, *412*, 809–812, doi:10.1038/35090552.

Hartley, G., and A. Mucci (1996), The influence of P_{CO2} on the partitioning of magnesium in calcite overgrowths precipitated from artificial seawater at 25° and 1 atm total pressure, *Geochim. Cosmochim. Acta*, *60*, 315–324, doi:10.1016/0016-7037(95)00388-6.

Keeling, R. F., and B. B. Stephens (2001), Antarctic sea ice and the control of Pleistocene climate instability, *Paleoceanography*, *16*, 330–334, doi:10.1029/2001PA000648.

Levitus, S., and T. Boyer (1994), *World Ocean Atlas*, U.S. Dept. of Commer., Washington, D. C. (Available at http://ingrid.ldeo.columbia.edu/SOURCES/.LEVITUS/)

Lisiecki, L. E., and M. E. Raymo (2005), A Pliocene-Pleistocene stack of 57 globally distributed benthic $\delta^{18}O$ records, *Paleoceanography*, *20*, PA1003, doi:10.1029/2004PA001071.

Loubere, P., and R. Chellappa (2008), Carbonate preservation in marine sediments: Mid to higher latitude quantitative proxies, *Paleoceanography*, *23*, PA1209, doi:10.1029/2007PA001470.

Lumsden, D. N. (1979), Discrepancy between thin-section and X-ray estimates of dolomite in limestone, *J. Sediment. Petrol.*, *49*, 429–436.

Lynch-Stieglitz, J., and R. G. Fairbanks (1994), Glacial-interglacial history of Antarctic intermediate water: Relative strengths of Antarctic versus Indian Ocean sources, *Paleoceanography*, *9*, 7–29, doi:10.1029/93PA02446.

Lyons, T. W., R. W. Murray, and D. G. Pearson (2000), A comparative study of diagenetic pathways in sediments of the Caribbean Sea: Highlights from pore-water results, *Proc. Ocean Drill. Program Sci. Results*, *165*, 287–298.

Malone, M. J. (2000), Data report: Geochemistry and mineralogy of periplatform carbonate sediments: Sites 1006, 1008, and 1009, *Proc. Ocean Drill. Program Sci. Results*, *166*, 145–152.

Malone, M. J., N. C. Slowey, and G. M. Henderson (2001), Early diagenesis of shallow-water periplatform carbonate sediments, leeward margin, Great Bahama Bank (Ocean Drilling Program Leg 166), *Geol. Soc. Am. Bull.*, *113*, 881–894, doi:10.1130/0016-7606(2001)113<0881:EDOSWP>2.0.CO;2.

McCorkle, D. C., P. A. Martin, D. W. Lea, and G. P. Klinkhammer (1995), Evidence of a dissolution effect on benthic foraminiferal shell chemistry: $\delta^{13}C$, Cd/Ca, Ba/Ca, and Sr/Ca results from the Ontong Java Plateau, *Paleoceanography*, *10*, 699–714, doi:10.1029/95PA01427.

Moberly, R. J. (1968), Composition of magnesian calcites of algae and pelecypods by electron microprobe analysis, *Sedimentology*, *11*, 61–82, doi:10.1111/j.1365-3091.1968.tb00841.x.

Morrison, J. M., and W. D. Nowlin (1982), General distribution of water masses within the eastern Caribbean Sea during the winter of 1972 and fall of 1973, *J. Geophys. Res.*, *87*, 4207–4229, doi:10.1029/JC087iC06p04207.

Morse, J. W., and R. S. Arvidson (2002), The dissolution kinetics of major sedimentary carbonate minerals, *Earth Sci. Rev.*, *58*, 51–84, doi:10.1016/S0012-8252(01)00083-6.

Morse, J. W., A. J. Andersson, and F. T. Mackenzie (2006), Initial responses of carbonate-rich shelf sediments to rising atmospheric pCO_2 and "ocean acidification": Role of high Mg-calcites, *Geochim. Cosmochim. Acta*, *70*, 5814–5830, doi:10.1016/j.gca.2006.08.017.

Mucci, A. (1987), Influence of temperature on the composition of magnesian calcite overgrowths precipitated from seawater, *Geochim. Cosmochim. Acta*, *51*, 1977–1984, doi:10.1016/0016-7037(87)90186-4.

Oomori, T., H. Kaneshima, Y. Maezato, and Y. Kitano (1987), Distribution coefficient of Mg^{2+} ions between calcite and solution at 10–50°C, *Mar. Chem.*, *20*, 327–336, doi:10.1016/0304-4203(87)90066-1.

Oppo, D. W., and R. G. Fairbanks (1990), Atlantic ocean thermohaline circulation of the last 150,000 years: Relationship to climate and atmospheric CO_2, *Paleoceanography*, *5*, 277–288, doi:10.1029/PA005i003p00277.

Pahnke, K., and R. Zahn (2005), Southern hemisphere water mass conversion linked with North Atlantic climate variability, *Science*, *307*, 1741–1746, doi:10.1126/science.1102163.

Paillard, D., L. Labeyrie, and P. Yiou (1996), Macintosh program performs time-series analysis, *Eos Trans. AGU*, *77*, 379, doi:10.1029/96EO00259.

Pailler, D., and E. Bard (2002), High frequency paleoceanographic changes during the past 140 000 yr recorded by the organic matter in sediments of the Iberian Margin, *Palaeogeogr. Palaeoclimatol. Palaeoecol.*, *181*, 431–452, doi:10.1016/S0031-0182(01)00444-8.

Paquette, J., and R. J. Reeder (1990), Single-crystal X-ray structure refinements of 2 biogenic magnesian calcite crystals, *Am. Mineral.*, *75*, 1151–1158.

Peeters, F. J. C., R. Acheson, G. J. A. Brummer, W. P. M. de Ruijter, R. R. Schneider, G. M. Ganssen, E. Ufkes, and D. Kroon (2004), Vigorous exchange between the Indian and Atlantic oceans at the end of the past five glacial periods, *Nature*, *430*, 661–665, doi:10.1038/nature02785.

Raisbeck, G. M., F. Yiou, O. Cattani, and J. Jouzel (2006), ^{10}Be evidence for the Matuyama–Brunhes geomagnetic reversal in the EPICA Dome C ice core, *Nature*, *444*, 82–84, doi:10.1038/nature05266.

Reijmer, J. J. G., and N. Andresen (2007), Mineralogy and grain size variations along two carbonate margin-to-basin transects (Pedro Bank, Northern Nicaragua Rise), *Sediment. Geol.*, *198*, 327–350, doi:10.1016/j.sedgeo.2007.01.018.

Ridgwell, A., and J. C. Hargreaves (2007), Regulation of atmospheric CO_2 by deep-sea sediments in an Earth system model, *Global Biogeochem. Cycles*, *21*, GB2008, doi:10.1029/2006GB002764.

Ridgwell, A., I. Zondervan, J. C. Hargreaves, J. Bijma, and T. M. Lenton (2007), Assessing the potential long-term increase of oceanic fossil fuel CO_2 uptake due to CO_2-calcification feedback, *Biogeosciences*, *4*, 481–492.

Sabine, C. L., et al. (2004), The oceanic sink for anthropogenic CO_2, *Science*, *305*, 367–371, doi:10.1126/science.1097403.

Schlager, W., and N. P. James (1978), Low-magnesian calcite limestones forming at deep-sea floor, Tongue of Ocean, Bahamas, *Sedimentology*, *25*, 675–702, doi:10.1111/j.1365-3091.1978.tb00325.x.

Schmidt, M. W., H. J. Spero, and D. W. Lea (2004), Links between salinity variation in the Caribbean and North Atlantic thermohaline circulation, *Nature*, *428*, 160–163, doi:10.1038/nature02346.

Schmidt, M. W., M. J. Vautravers, and H. J. Spero (2006), Western Caribbean sea surface temperatures during the late Quaternary, *Geochem. Geophys. Geosyst.*, *7*, Q02P10, doi:10.1029/2005GC000957.

Schmitz, W. J., and P. L. Richardson (1991), On the sources of the Florida current, *Deep Sea Res.*, *38*, suppl., 379–409.

Sepulcre, S. (2008), Essais de datations absolues et reconstitutions paléoclimatiques en Mer des Caraïbes: Approche multitraceurs sur les foraminifères planctoniques et la fraction fine aragonitique, Ph.D. thesis, 368 pp., Aix-Marseille Univ., Aix-en-Provence, France.

Sepulcre, S., K. Tachikawa, L. Vidal, and E. Bard (2007), Large ^{14}C age offsets between fine aragonite fraction and coexisting planktonic foraminifera in shallow Caribbean sediments, *Geochim. Cosmochim. Acta*, *71*(15), suppl. S1, A917.

Sepulcre, S., N. Durand, and E. Bard (2009), Mineralogical determination of reef and periplatform carbonates: Calibration and implications for paleoceanography and radiochronology, *Global Planet. Change*, *66*, 1–9, doi:10.1016/j.gloplacha.2008.07.008.

Stanley, S. M., and L. A. Hardie (1998), Secular oscillations in the carbonate mineralogy of reef-building and sediment-producing organisms driven by tectonically forced shifts in seawater chemistry, *Palaeogeogr. Palaeoclimatol. Palaeoecol.*, *144*, 3–19, doi:10.1016/S0031-0182(98)00109-6.

Tachikawa, K., S. Sepulcre, T. Toyofuku, and E. Bard (2008), Assessing influence of diagenetic carbonate dissolution on planktonic foraminiferal Mg/Ca in the southeastern Arabian Sea over the past 450 ka: Comparison between *Globigerinoides ruber* and *Globigerinoides sacculifer*, *Geochem. Geophys. Geosyst.*, *9*, Q04037, doi:10.1029/2007GC001904.

Toggweiler, J. R., and B. Samuels (1998), On the ocean's large-scale circulation near the limit of no vertical mixing, *J. Phys. Oceanogr.*, *28*, 1832–1852, doi:10.1175/1520-0485(1998)028<1832:OTOSLS>2.0.CO;2.

Tomczak, M., and J. S. Godfrey (2003), *Regional Oceanography: An Introduction*, 2nd ed., 390 pp., Am. Meteorol. Soc., Boston, Mass.

Toyofuku, T., H. Kitazato, H. Kawahata, M. Tsuchiya, and M. Nohara (2000), Evaluation of Mg/Ca thermometry in foraminifera: Comparison of experimental results and measurements in nature, *Paleoceanography*, *15*, 456–464, doi:10.1029/1999PA000460.

Valet, J.-P., L. Meynadier, and Y. Guyodo (2005), Geomagnetic field strength and reversal rate over the past two million years, *Nature*, *435*, 802–805, doi:10.1038/nature03674.

Verardo, D. J., P. N. Froelich, and A. McIntyre (1990), Determination of organic carbon and nitrogen in marine sediments using the Carlo-Erba-Na-1500 analyzer, *Deep Sea Res., Part A*, *37*, 157–165.

Wolff, T., S. Mulitza, H. Arz, J. Patzold, and G. Wefer (1998), Oxygen isotopes versus CLIMAP (18 ka) temperatures: A comparison from the tropical Atlantic, *Geology*, *26*, 675–678, doi:10.1130/0091-7613(1998)026<0675:OIVCKT>2.3.CO;2.

Wüst, G. (1964), *Stratification and Circulation in the Antillean-Caribbean Basins*, 201 pp., Columbia Univ. Press, New York.